Waste and Biomass Valorization (2023) 14:2085–2101
https://doi.org/10.1007/s12649-022-01996-3

ORIGINAL PAPER

Structure and Properties of Lignin Extracted from Cotton Stalk by Non-polluting Ethanol-Assisted Hot Water Pretreatment and its High-Value Utilization for Methylene Blue Removal

Tao Yang[1,2] · **Zhiyi Li**[1] · **Wei Wei**[1] · **Xiaojuan Wang**[1] · **Fengxia Liu**[1] · **Xiaofei Xu**[1] · **Zhijun Liu**[1]

Received: 27 July 2022 / Accepted: 19 November 2022 / Published online: 8 December 2022
© The Author(s), under exclusive licence to Springer Nature B.V. 2022

Abstract

Lignin has a unique chemical structure that can effectively adsorb dye cations in sewage. In this paper, a non-polluting ethanol-assisted hot water pretreatment method was used to extract lignin from the cotton stalk. The structure and properties of lignin were investigated, and the adsorption isotherm model, internal diffusion model, and adsorption kinetic equation for the adsorption of methylene blue were verified. The extraction yield of lignin was 15.65%. The molecular mass of lignin was only about 900 Da. Both Infrared Spectroscopy and 2D-Nuclear Magnetic Resonance showed that it contained the type of grass lignin units (guaiacyl, syringyl, and p-hydroxyphenyl) phenolic hydroxyl units. The morphology of the lignin was that there were many burr particles on the blocky surface. The lignin had a good effect in removing methylene blue, with 17.11 mg/g, and its pH range was wide from 3 to 8. The Dubinin–Radushkevich model is the best isothermal model that matches the experimental data, $R^2 = 0.988$, the pseudo-second-order kinetic equation is the best-matching model, $R^2 = 0.9369$. In the intraparticle diffusion model test, intra-particle diffusion occurs in the second stage of the matching line.

Graphical Abstract

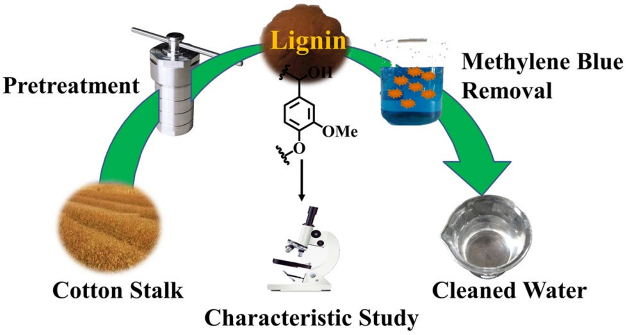

Keywords Hot water pretreatment · Cotton stalk · Lignin · Adsorption · Methylene blue

Statement of Novelty

Cellulose, hemicellulose, and lignin contained in a large number of the discarded cotton stalk can be favored as raw materials. In this paper, we used the ethanol solution-assisted hot water method to extract the lignin. And the lignin had a low molecular weight of 846–989 Da. This lignin was a typical grass lignin with a G, S, and H aromatic structure, and its thermal stability was no different from other lignins.

✉ Zhijun Liu
liuzj@dlut.edu.cn

[1] R&D Institute of Fluid and Powder Engineering, Dalian University of Technology, Dalian 116024, China

[2] School of Chemical Engineering and Technology, Xinjiang University, Urumqi 830046, China

However, the lignin particles obtained by this method had burr protrusions on the surface, which made them have good acid resistance when adsorbing methylene blue. The pH range of its adsorption of methylene blue was 3–8.

Introduction

Due to the environmental impact and the fossil energy depletion crisis, the use and development of green and sustainable chemical raw materials have been paid more and more attention. Biomass energy has always been sustainable green energy for people's survival, development, and utilization [1]. Lignocellulosic biomass is mainly composed of carbohydrate polymers (cellulose and hemicellulose), and aromatic polymers (lignin and tannin) [2]. As an annual herb commercial crop, cotton is widely grown worldwide, and the output reached 25.5 million tons in 2011 [3]. And the waste reaches about 35 million tons every year [4]. Cotton stalks, the most productive waste, are usually crushed and spread on arable land, which damages the soil structure [5]. So people have begun to focus on converting it into industrial feedstock for use. For example, after hot water pretreatment of cotton stalk, the hemicellulose is degraded into five-carbon monosaccharides, which can be used for making furfural and hydroxymethylfurfural [6–10]. And cellulose can be used in many regions like the 3D printing field and some carbon sources [11–13]. The chemical structure of lignin consists of the amount of phenylpropane units (p-hydroxyphenyl (H), guaiacyl (G), syringyl (S)), and a large number of carboxyl and hydroxyl groups [14]. The unique structure of lignin can adsorb some heavy metal cations and dye cations in solution [15–19].

A large amount of dyes wastewater comes from the booming printing and dyeing industry, and this wastewater has become a thorny environmental pollution problem in many places because they threaten human healthy by carcinogenicity, mutagenicity, teratogenicity, non-degradability [15, 20–24]. At present, the main technologies for treating dyes wastewater are flocculation, oxidation, adsorption, coagulation, and photocatalysis [25–29]. Oxidation takes a long time and will produce secondary pollution such as unpleasant odor, high requirements for photocatalytic equipment, and high requirements for the flocculation of raw materials [30]. Adsorption is favored by people because of its simplicity and ease of operation, wide material sources, and low secondary pollution [27, 31, 32]. As lignin contains C = O and –OH, it will react with dye ions to achieve the purpose of adsorbing dyes [33–35].

As a low-cost and non-pollution method to remove or extract hemicellulose from biomass, hot water pretreatment has been favored by researchers [36, 37]. Xylitol and furfural are the main products of hemicellulose decomposition [38]. And the hot water pretreatment also promoted lignin extraction [39]. Then the lignin could be extracted by the organosolv method which promotes lignin decomposition. And the molecular mass of lignin would be small [40]. Mechelin et al. reported that they adopted this method to treat corn stalks and obtained high yield and purity lignin [41]. We believe that this two-step process is the optimal method to refine biomass in the future, so this paper also adopts the method to treat cotton stalks and obtained small molecular mass lignin with high purity. Besides we also studied its structure and performance on adsorption methylene blue, looking forward to realizing high-value utilization of lignin without pollution.

Materials and Methods

Materials

The cotton stalk was obtained from Xinjiang Fukang in China. The cotton stalk was cleaned several times with tap water to clean the dirt, then washed with deionized water 3 times, and dried for 10 h at 105 ℃ by blast drying oven (Yi Heng, China). Then, the cotton stalk was crushed into particles (Lingsum grinder, 3.2 kW) and sieved through 40 meshes. The compositions (wt%) of the cotton stalk were determined by the Van Soest Biomass Analysis Method as shown in Table 1 [42].

Table 1 The composition of the cotton stalk and HW particles

Components	Cotton stalk %(w/w)	HW residue solid of cotton stalk % (w/w)
Cellulose	35.13 ± 2.13	59.46 ± 2.35
hemicellulose	22.87 ± 2.42	4.78 ± 2.48
Lignin	18.16 ± 0.15	34.45 ± 2.14
Ashes	6.92 ± 0.93	–

Extraction of Lignin

The extraction processes were divided into two steps: the first step was hot water (HW) pretreatment; the second step was the organosolv method, using the ethanol aqueous solution to extract lignin at different temperatures. The process was shown schematically in Fig. 1.

Hot Water Pretreatment

In the first stage, cotton stalk particles and deionized water were put into a 500 mL stainless steel reactor (316 L) at the designed solid–liquid ratio (w/v,1/5–1/15) and heated up to 180–200 ℃, hold for 30–60 min, designed by Orthogonal

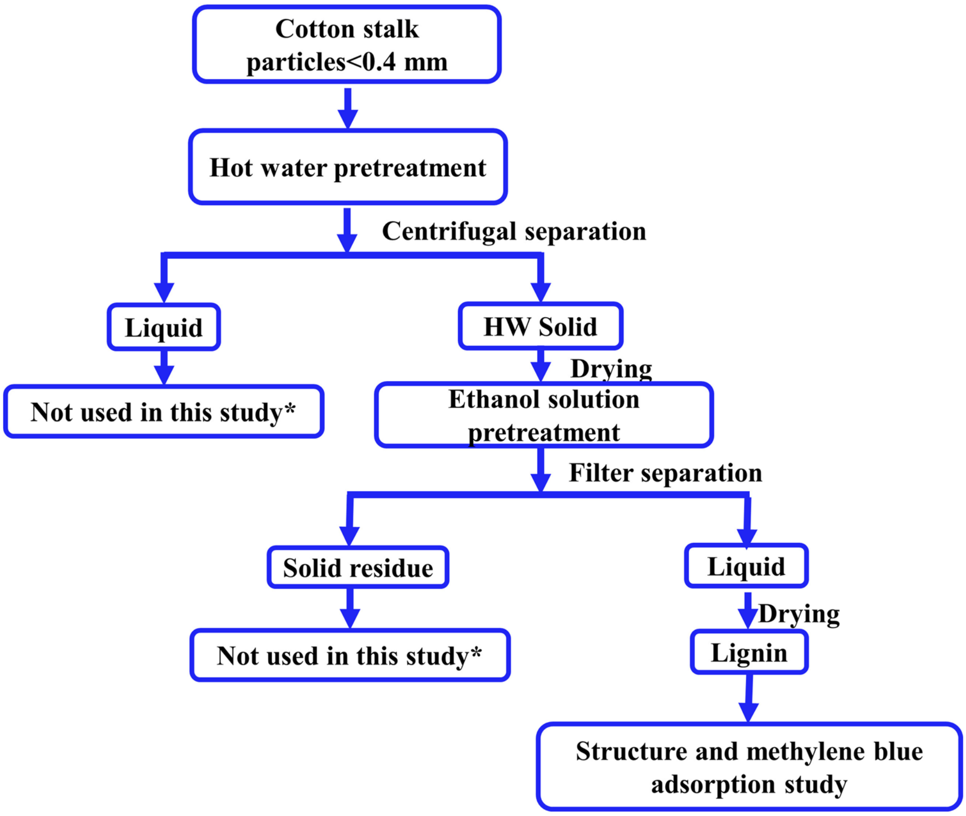
Cotton stalk particles<0.4 mm
Hot water pretreatment
Centrifugal separation
Liquid
HW Solid
Drying
Not used in this study*
Ethanol solution pretreatment
Filter separation
Solid residue
Liquid
Drying
Not used in this study*
Lignin
Structure and methylene blue adsorption study

Fig. 1 Schematic process for extraction lignin from cotton stalk

Table 2 Orthogonal experiments on hemicellulose residues of HW particles

Sample	Temperature (℃)	Solid-water Ratio	Time (min)	Hemicellulose Residual (%)	HW-solid Yield (%)
1	180	5	30	9.04 ± 1.36	57.66 ± 2.33
2	180	10	60	8.57 ± 2.02	61.24 ± 3.12
3	180	15	45	8.42 ± 1.87	59.88 ± 1.66
4	190	5	60	7.36 ± 2.76	60.74 ± 3.24
5	190	10	45	6.88 ± 2.77	59.57 ± 2.66
6	190	15	30	7.02 ± 3.02	58.49 ± 3.78
7	200	5	45	7.14 ± 1.94	59.32 ± 2.19
8	200	10	30	6.92 ± 2.88	60.67 ± 2.72
9	200	15	60	6.53 ± 3.24	61.76 ± 3.03
Actual	200	15	30	6.74 ± 2.87	58.56 ± 2.72

Experiment as shown in Table 2, then cooled down to room temperature with cold water. The hot water (HW) particles yield was calculated by the following Eq. (1):

$$Y_{LHW} = \frac{m_{LHW}}{m_{cotton}} \times 100\% \tag{1}$$

where the Y_{HW} represented the yield of HW particles, m_{HW} was the mass of HW particles, and m_{cotton} was the mass of cotton stalk particles. The products were separated by filter paper to obtain the HW particles that were washed with distilled water at 100 °C 3 times and dried at 105 ℃. The components of the filtrate were mainly hemicellulose derivatives like xylose, arabinose, and some soluble lignin [41].

Organoslv Method

The HW particles (2 g) were put into a 150 mL stainless steel reactor (316 L), and 10 mL ethanol solution (40–80%) was loaded into the reactor. Then the reactor was heated up to the preset temperature (180–220 ℃) designed by SPSS software (IBM, American) as shown in Table 3, and kept for 1–3 h, during the process lignin was precipitated from the HW particles and dissolved into the solvent. The lignin yield was accounted for by Eq. (2):

$$Y_{lig} = \frac{m_{lig}}{m_{LHW}} \times 100\% \tag{2}$$

where the Y_{lig} represented the lignin extracted efficiency from HW particles, m_{lig} was the mass of lignin, and m_{HW} was the mass of HW particles. Then the reactor was cooled down to room temperature with cold water. After that, collected the solid–liquid mixture in the reactor, then separated

Table 3 The variance analysis of orthogonal experiments of removing hemicellulose hydrolyzed by HW

Source	Type III sum of square	df	Mean square	F	Sig value
Correct model	6.372	6	1.062	134.818	0.007
Interact	511.966	1	511.966	64,988.638	0.000
Temperature	5.866	2	2.933	372.323	0.003
Ratio	0.444	2	0.222	28.165	0.034
Time	0.062	2	0.031	3.966	0.201
Error	0.016	2	0.031		
Total corrected	518.354	9	0.008		
Total	6.388	8			

with filter paper. At last, collected the filtrate and rinsed the residue with ethanol.

Lignin Charactersization Analysis

Thermal Stability of Lignin

As an amorphous polymer, lignin is a typical thermoplastic material [43]. The decomposition temperature (Td) was analyzed by Mettler thermal analyzer. About 16 mg of lignin particles are placed in the crucible. Then the temperature was heated up to 800 °C, 10 °C/min, accompanied by nitrogen flow.

Gel Permeation Chromatography

Acetylation of lignin particles before molecular mass determination. About 0.1 g lignin powder dissolved in 1 mL pyridine, then added 1 mL acetic anhydride, was mixed well in the darkroom and stood for 24 h. Then added ethanol to the wash, spun steam to remove the acetylation reagent, and froze dry. The acetylated lignin was dissolved in Tetrahydrofuran (THF) and filtered through a 0.2 μm syringe filter. The sample concentration was about 0.1%, and the injection volume was 50 μL.

Molecular mass distributions of copolymers were measured by Agilent High-Temperature Gel Permeation Chromatograph (PL-GPC 220) at 30 ℃ and a flow rate of 1.0 mL/min with THF as the eluent. The curve was calibrated using monodisperse polystyrene standards covering the molecular mass range from 580 to 460,000 Da.

Infrared Analysis

Infrared detection is an effective detection method that can distinguish the functional groups mentioned above. The detective method was that the lignin samples were milled with KBr (1:100), and analyzed from 4500 to 500 cm^{-1} at a resolution of 4 cm^{-1} and 16 scans by Fourier Transform Infrared technique (Thermo Fisher).

Scanning Electron Microscopy Test

The surface of the lignin sample was observed by Scanning Electron, (FEI QUANTA 450, American). The sample needs to be groundand sprayed with gold. The magnification required for observation was 2000 × and 5000 × respectively.

2D-HSQC NMR Analysis

Dried lignin pariticles (120 mg) were placed in a 5 mm NMR tube, 0.7 mL of DMSO-d_6 was added, and ultrasonically oscillated for 30 min to mix well. The test analysis instrument was Bruker AVANCE III 500, test conditions: temperature 25 °C; pulse angle: 30°; sampling time (AQ) = 13.6 s, delay time (Dl) 3.98 s; the number of scans (NS) 30,000 times. The spectral widths of 5000 Hz and 20,000 Hz correspond to the dimensions of the ^{1}H and ^{13}C spectra, respectively, $J_{(\delta C-\delta H)}$ was set to 140 Hz, and the solvent DMSO peak (δC 39.5; δH 2.50) was set to the shift of the TMS.

Specific Surface Area and Pore Size Test

Specific surface area and the pore size of the cotton stalk lignin were determined using the Brunauer, Emmett, and Teller (BET) and the Barret, Joyner, and Halenda (BJH) methods in a surface area analyzer from Beishide Instruments (China). About 200 mg of dried lignin was maintained at 110 °C under vacuum for 24 h to remove moisture and other volatile compounds that could be adsorbed on the surface of the sample. The adsorption and desorption isotherms of N_2 by the sample at 77.3 K were obtained using relative vapor pressures (P/P_0) from 0.0116 to 0.0984.

Methylene Blue Adsorption

The methylene blue (MB) ($C_{16}H_{18}C_lN_3S \cdot 3H_2O$) purchased from the Macklin company was prepared with different concentrations, building a standard curve (from 20 to 200 mg L^{-1}) at 664 nm UV (Shimadzu, UV-1800, Japan). The R^2 between the experimental point and the standard curve reached 0.99. The followingexperiments were repeated 3–5 times to ensure the error was within 10%.

Methylene Blue Adsorption Capacity Study

The specific experimental parameters were that the lignin dosage was from 30 to 300 mg, and the stirring frequency was from 90 to 210 rpm. Then the ground lignin particles were added to the MB solution (10 mL, 100 mg L^{-1}) and shaken for 8 h. The adsorption process was evaluated in terms of two response variables: the adsorption capacity of the MB by the lignin sample (q_t, mg g^{-1}) and the percentage of MB removal (R, %). These variables were calculated using Eq. (3) and Eq. (4), respectively [43].

$$q_t = \frac{(C_0 - C_t)}{m}V \tag{3}$$

$$\%R = \frac{(C_0 - C_t)}{C_0} \times 100 \tag{4}$$

where q_t is the amount of MB retained per gram of lignin as a function of time (mg g^{-1}), C_0 and C_t are the initial concentration and the concentration at time t, respectively, of MB (mg L^{-1}), V is the volume (L).

The Adsorption Isotherm Model Study

The adsorption isotherm model is mainly evaluated by four nonlinear models: Freundlich [44], Langmuir [45], and Temkin and Dubinin–Radushkevich [43], these models parameters should be adjusted by adsorption experimented data. The initial concentration of MB was 375 mg L^{-1}, and the lignin mass was 150 mg, their contact time was 12 h under 150 rpm stirring frequency at 25 ℃.

The expression of the Freundlich model in Eq. (5):

$$q_e = k_F c_e^{1/n} \tag{5}$$

where the q_e is the q_t value of lignin when adsorption reaches equilibrium, the k_F (mg g^{-1} (mg L^{-1}) $^{-1/n}$) and n are constants that depend on the temperature and are related to the adsorption capacity and intensity, c_e is the concentration of equilibrium of MB (mg L^{-1}).

The equation of the Langmuir model is expressed as Eq. (6):

$$q_e = \frac{q_m k_L c_e}{1 + k_L c_e} \tag{6}$$

where the q_e is the q_t value of lignin when adsorption reaches equilibrium (mg g^{-1}), the q_m is the maximum theoretical adsorption capacity that corresponds to a monolayer covering (mg g^{-1}), and k_L is the Langmuir isothermal constant (L mg^{-1}), C_e is the concentration of equilibrium of MB (mg L^{-1}).

The equation of the Temkin model is expressed as Eq. (7):

$$q_e = \frac{RT}{b_t}\ln(A_t c_e) \tag{7}$$

where the q_e is the q_t value of lignin when adsorption reaches equilibrium (mg g^{-1}), R is the constant 8.314 (JK^{-1} mol^{-1}), T is the temperature (K), the b_t is the maximum theoretical heat of adsorption (J mol^{-1}), A_t is the equilibrium binding constant (L mg^{-1}) that corresponds to the maximum binding energy, c_e is the concentration of equilibrium of MB (mg L^{-1}).

The equation of the Dubinin–Radushkevich model is expressed as Eqs. (8) and (9):

$$q_e = q_s \exp(k_{ad}\varepsilon) \tag{8}$$

$$\varepsilon = RTln(1 + \frac{1}{c_e}) \tag{9}$$

where the q_e is the q_t value of lignin when adsorption reaches equilibrium (mg g^{-1}), R is the constant 8.314 (JK^{-1} mol^{-1}), T is the temperature (K), q_s is the adsorption capacity (mg g^{-1}), k_{ad} is a constant related to the sorption energy (mol^2 J^{-2}), ε is the Polanyi potential (kJ mol^{-1}).

Study on Adsorption Kinetics and Intra-particle diffusion of MB

To study the adsorption kinetics of lignin on MB, 70 mg lignin was placed in 25 mL of different concentration MB solution (120–200 mg L^{-1}), shaking at 150 rpm for 12 h. The adsorption kinetics was evaluated using two models, the pseudo-first-order (PFO) model [46] and the pseudo-second-order model (PSO) [47], the equations are expressed as Eqs. (10) and (11):

$$q_t = q_e(1 - e^{-k_1 t}) \tag{10}$$

$$q_t = \frac{q_e^2 k_2 t}{1 + k_2 q_e t} \tag{11}$$

where the q_e is the q_t value of lignin when adsorption reaches equilibrium (mg g^{-1}), q_t is the amount of adsorption of MB at time t (mg g^{-1}), k_1 is the PFO constant (min^{-1}) and k_2 is the PSO constant (g mg^{-1} min^{-1}), t is the contact time (min).

The form of adsorption and diffusion of methylene blue cations in lignin pores is calculated by the Weber-Morris intra-particle diffusion model, the equation is expressed as Eq. (12):

$$q_t = k_3 t^{0.5} + C \tag{12}$$

where k_3 is the constant of intra-particles diffusion, t is the time, and C is the intercept of the fitting line.

Effect of pH and Determination of PZC

The initial pH value was changed from 2 to 11 using NaOH (0.1 mol L^{-1}) and HCl (0.1 mol L^{-1}) solutions for the pH adjustment. The pH value was detected by a pH meter (METTLER TOLEDO, Switzerland). In this study, 225 mg lignin was placed in 50 mL of 100 mg L^{-1} MB solution. shaken at 150 rpm for 480 min at 25 ℃.

The pH at the zero charge point (pHPZC) was measured following: about 0.1 g lignin was placed in a 100 mL Erlenmeyer flask included in 50 mL NaCl (0.1 mol L^{-1}) solution. And then changed the pH value from 2 to 11 using NaOH (0.1 mol L^{-1}) and HCl (0.1 mol L^{-1}) solution, shaken at 150 rpm for 24 h at 25 ℃ [48, 49].

Results and Discussion

The Composition of the Cotton Stalk and HW Particles

The composition of cotton stalk analyzed by the Van Soest Biomass Method is shown in Table 1, the cellulose content is about 35.12%, the lignin content is about 18.16% and the hemicellulose content is about 22.87%. The results obtained by this method are similar to the results obtained by NREL analysis [50].

The purpose of the HW process in this experiment was to remove hemicellulose, hydrolyze it into monosaccharides, and leave lignin and cellulose in the next stage for processing. The hydrolyzed products of hemicellulose were xylose and arabinose [51]. The low content of residual hemicellulose was the target of orthogonal experiments designed by SPSS software for hot water pretreatment. The experimental conditions are shown in Table 2, the temperature is from 180 to 220 °C, the time is from 30 to 60 min, and the solid–liquid ratio (w/v) is from 1/5 to 1/15. After calculating the variance in Table 3, it is found that the Sig value of temperature and solid–liquid ratio are both less than 0.05, which indicates that these two parameters are extremely important for the experiment, while the Sig value of time is larger than 0.05, indicating that time is not a necessary option for this experiment. Therefore, the optimal condition of hot water for removal of hemicellulose is 200 °C, the solid–liquid ratio (w/v) 1/15 and 30 min. It can be seen that the content of hemicellulose in HW particles is reduced to 6.74% after hot water pretreatment, and the HW solid yield was about 58.56%.

The Lignin Yield and its Molecular Mass Determination

The method of extracting lignin with ethanol solution in the second stage also used SPSS software to design orthogonal experiments and the experimental goal was to get a high lignin yield. The experimental conditions and lignin yield are shown in Table 4. The Sig value in Table 5 shows that both temperature and ethanol content is less than 0.05, while the Sig value of time is larger than 0.05, which means that temperature and ethanol content is truly significant parameters, but time is not, finally, the best experiment condition is 220 ℃, the ethanol content 80% and 1 h. The lignin yield obtained under this optimum condition is 15.65%, and its purity is 88.98%.

Figure 2 is the molecular mass test of lignin. Interestingly, the molecular mass gradually decreases with the increase in temperature (989 Da, 937 Da, 846 Da), which directly indicates that the lignin is degraded during the extraction process. Sun et al. reported that the molecular mass of lignin is 530–1100 Da, which is consistent with our study [52].

Table 4 Orthogonal experimental design on the extraction of lignin by ethanol solution

Sample	Temperature (℃)	Ethanol content (%)	Time (h)	Lignin yield (%)	Lignin purity (%)
1	180	40	1	8.23 ± 1.32	81.22 ± 2.35
2	180	60	3	9.23 ± 2.24	87.44 ± 1.21
3	180	80	2	9.51 ± 3.01	90.14 ± 2.19
4	200	40	3	10.61 ± 2.76	79.83 ± 2.74
5	200	60	2	11.74 ± 1.89	82.66 ± 3.52
6	200	80	1	12.75 ± 2.56	89.27 ± 2.28
7	220	40	2	15.06 ± 3.11	83.73 ± 5.36
8	220	60	1	14.56 ± 2.79	91.38 ± 4.62
9	220	80	3	16.33 ± 1.96	87.33 ± 4.58
Actual	220	80	1	15.65 ± 2.77	88.98 ± 3.67

Table 5 The variance analysis of orthogonal experiments of extraction lignin

Source	Type III sum of square	df	Mean square	F	Sig value
Correct Model	0.03	6	0.005	169.464	0.006
Interact	0.533	1	0.533	18,136.198	0.000
Temperature	0.028	2	0.014	481.618	0.002
Ratio	0.002 5.470E-5	2	0.001	25.843	0.037
Time	5.873E-5 0.562	2	2.735E-5	0.931	0.518
Error	0.03	2	2.936E-5		
Total corrected		9			
Total		8			

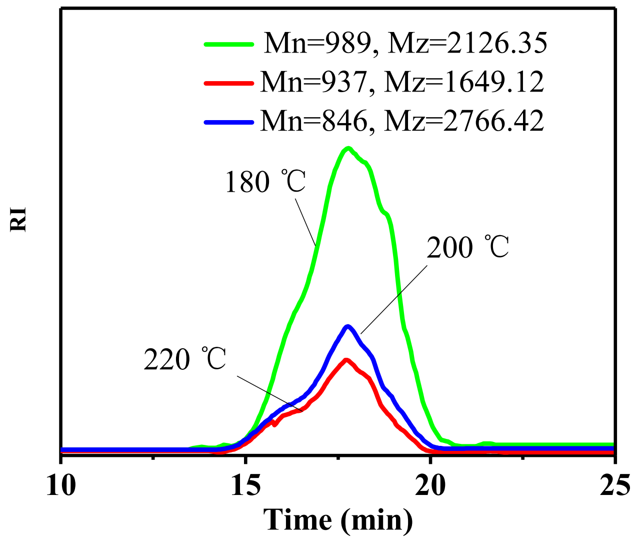

Fig. 2 The molecular mass and its distribution of lignin from ethanol extraction at 180–220 ℃

The Characteristic of Thermal Stability of Lignin Powder

The thermal stability of lignin was tested by the Mettler thermal analyzer. The mass loss rate was described as the blue curve shown in Fig. 3, the whole process was divided into three processes: the first stage was the volatilization process of water and small molecular substances [41]; the second process was the fast stage from 120 to 230 ℃, and the breaking bond was very violent [41]. The change in the third stage was the transformation process of the carbon–carbon bond breaking, and the chemical change became gentle. The red curve is represented the mass loss of lignin, it's divided into two stages, the first stage is from room temperature to 157 ℃. This stage is mainly the loss of small molecular substances, such as moisture and acids [41]. The second stage is the breaking of various chemical bonds, from carbon-hydrogen bonds to carbon–carbon bonds [41].

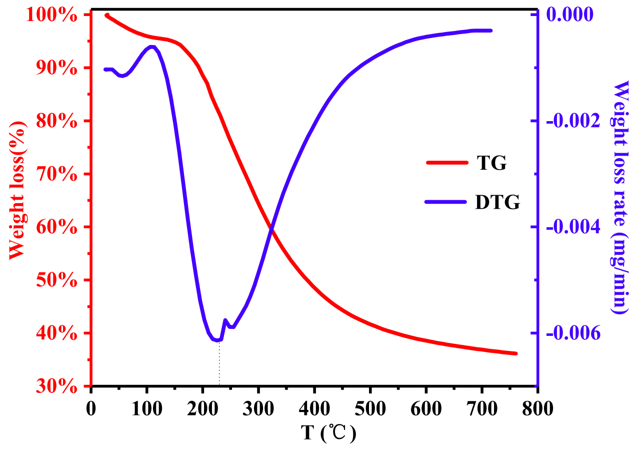

Fig. 3 The lignin thermal stability test (TGA)

The FT-IR Analysis of Lignin

Infrared spectroscopy analysis is an effective way to analyze the chemical structure and functional group composition of lignin. Judging the type of lignin can be easily obtained from the infrared spectrogram combined with previous literature. As shown in Fig. 4, it is clear that the absorption shoulders in the spectra have relatively similar spectral line profiles and intensities, indicating that a similar structure of the lignin fractionated from the cotton stalk obtained from 180 to 220 ℃ [53, 54]. That the 3448 cm^{-1} represented the –OH stretching vibration, 2954 cm^{-1}, and 2863 cm^{-1} was the C–H stretching vibration signal, and the 1700 and 1670 cm^{-1} was the C=O stretching vibration in carboxylic acids, aldehydes, and ketones [53–55]. At the fingerprint area, 1600, 1515, and 1423 cm^{-1} were assigned to the aromatic ring vibration [53, 54]. The 1460 cm^{-1} was attributed to the C–H deformation vibration of $–CH_2–$, $–CH_3$ combined with aromatic skeletal vibration [41]. 1365 cm^{-1} was the C–H deformation vibration signal, 1214 cm^{-1} was accused by C–O spatial deformation and the 1150 cm^{-1} was also caused by the C–H out-plane deformation, the 1118 cm^{-1} was caused by the O–H and C–O stretching vibration, the 1037 cm^{-1} was attributed to the ether bond in ring skeleton

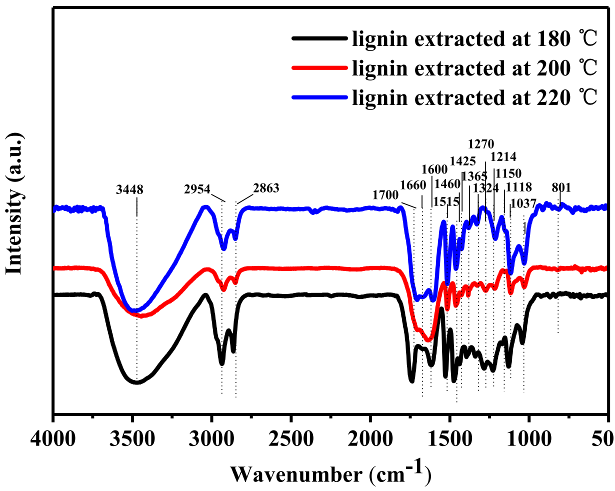

Fig. 4 The FT/IR spectra of lignin were extracted at different temperatures

vibration, 801 cm^{-1} was the signal of C–H out-plane vibration [53, 54]. The band around 1324 cm^{-1} was the signal of syringyl ring (S) breathing with C–O stretching, and the band around 1270 cm^{-1} was the signal of guaiacyl ring (G) breathing with C–O stretching [41].

2D-HSQC NMR Analysis

To better identify the structure of the cotton stalk lignin, the 2D-HSQC NMR was used to determine the chemical bonds of lignin. It was found that the products extracted from different temperatures were shown in Figs. 5 and 6. Figure 5 is the oxygenated aliphatic region δC/ δH 50–90/2.8–5.0 ppm area. The green part (-OME) at δC/δH 53.5/3.07 ppm is the signal of the methoxy group (OCH_3) in all pictures which is consistent with Sun's report [40]. The red color area marked Aγ observed at δC/δH 59.6/3.**7** ppm **is** related to the Cγ–Hγ in β-O-4' linkages in the A unit. And the pink area at δC/

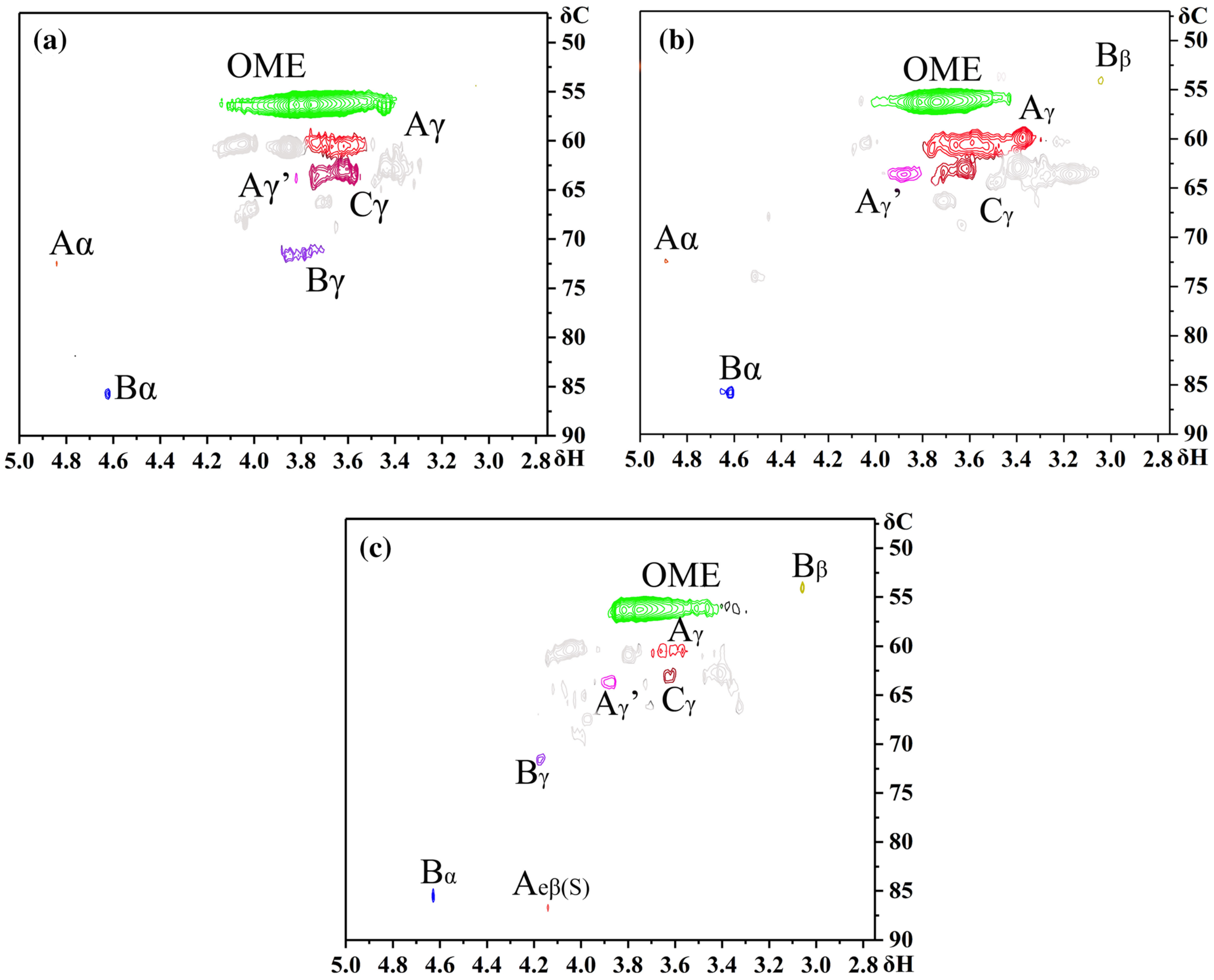

Fig. 5 HSQC-NMR spectra of cotton stalk lignin at the oxygenated aliphatic region δC/δH 50–90/2.8–5.0 ppm

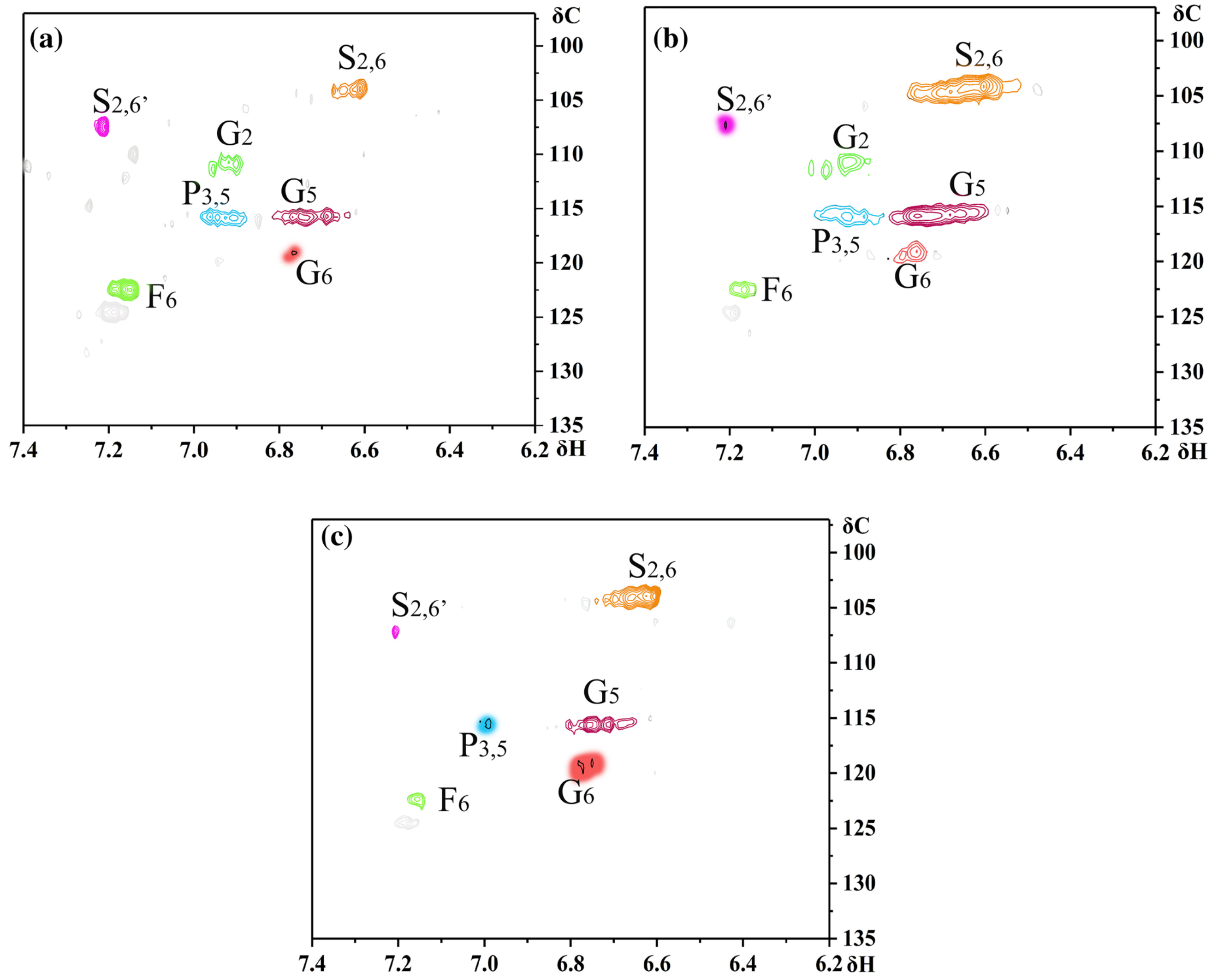

Fig. 6 HSQC-NMR spectra of cotton stalk lignin at aromatic region δC/δH 95–135/6.2–7.4 ppm

δH 63/3.9 ppm is correlated to the Cγ–Hγ in β-O-4’ linkages in the A’ unit which indicates that the lignin is slightly acetylated and the position of acetylation is in the γ position as shown in the A' unit in Fig. 7 [40]. The purple dotted area marked Aα in Fig. 5a, b at δC/δH 72.2/4.9 ppm is correlated to the Cα–Hα in β-O-4’ linkages in the S unit [56]. The orange dotted region marked as Aeβ(S) in Fig. 5c, the δC/δH 86.0/4.1 ppm region is the signal region of C_{β}–H_{β} correlated to the S-type β-O-4' substructure erythro of the A unit [40, 57]. The blood-red region marked Bγ, observed at the δC/δH 70.9/3.8 ppm in Fig. 5b, c is the signal of β–β’ correlated to the Cγ–Hγ in the B unit in Fig. 7 [40, 58]. The region observed at the δC/δH 53.5/3.07, 85.5/4.67, 63.3/3.74 ppm attributed to the β-B, α-B, and γ-C positions is also tested in the spectrum [56].

Figure 6 is the aromatic region of the HSQC spectrum of lignin, which mainly reveals the information of C and H on the benzene ring. The region δC/δH 104.3/6.7, 106.3/7.3 ppm marked $S_{2,6}$ and $S_{2,6}$’ represent $C_{2,6}$-$H_{2,6}$ in Cα-oxidized in S unit [40, 59]. The regions marked G_2, G_5, and G_6 observed at δC/δH 11.2/6.9, 114.7/6.7, and 119.4/6.75 ppm are correlated to C_2–H_2, C_5–$H_{5,}$ and C_6–H_6 in the G unit shown in Fig. 7. The light blue region marked $P_{3,5}$ at δC/δH 115/6.95 ppm is the signal of the $C_{3,5}$–$H_{3,5}$ belonging to the p-coumarate ester. The blue area marked F_6 at the δC/δH 122.5/7.15 ppm represents the C_6–H_6 correlation for ferulic acid ether structure in the H unit in Fig. 7 [52].

The Morphological Characteristics of Lignin Particles Tested by SEM

The morphological lignin particles were tested by Scanning Electron Microscopy. Since the morphology after extraction

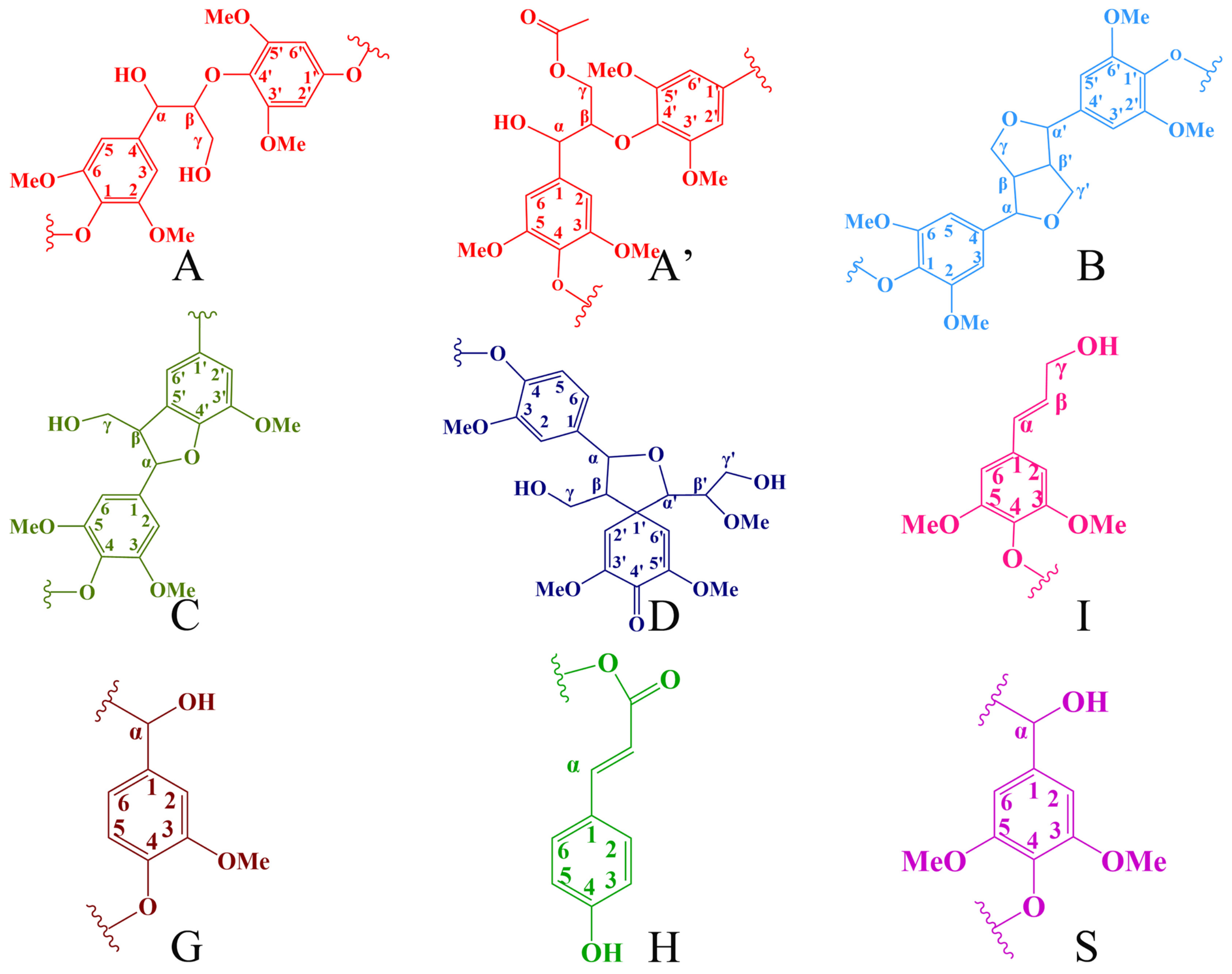

Fig. 7 Main structures present in cotton stalk lignin: **A** β-O-4'linkages; (A') γ-acetylated β-O-4' substructures; **B** retinol structures formed by β-β'/α-O-γ'/γ-O-α linkages; **C** phenyl coumarin structures formed by β-5/α-O-4 linkages; **D** spirodienone structures formed by β-1'/α-O-α linkages; **I** p-hydroxycinnamyl alcohol end-groups; **G** guaiacyl units; **H** p-hydroxyphenol (S) syringyl units

was similar, the lignin extracted at 220 °C was taken as an example. When the morphology of lignin powder is magnified 2000 times as shown in Fig. 8a, lignin particles are aggregated together in irregular lumps, and a lot of burrs can be observed on the edge of the lumps, and its surface is not smooth. When these small bumps are magnified to 5000 times shown in the circle part in Fig. 8b, it can be seen that many small fragments are piled up near the large lignin, and there are obvious boundaries or gaps between these small fragments. The existence of these burrs enables lignin to have a large surface area and can physically adsorb some substances, such as metal cations and dye cations.

The aggregation process of lignin occurred during the ethanol rotary evaporation, and a partial block formation could be seen at the bottom of the container. The higher the concentration, the deeper the agglomeration.

Specific Surface Area (BET) and Pore Size (BJH)

In addition, lignin also is a certain porosity, which makes lignin have certain physical adsorption properties. Figure 9 is the N_2 adsorption and desorption curves of lignin when calculating the specific surface area. The form of the curve is approximated to type V, according to the International Union of Pure and Applied 3 Chemistry (IUPAC) [60], which indicated that the cotton stalk lignin was mesoporous material.

Table 6 lists the specific surface area of cotton stalk lignin. The specific surface calculated by the BJH method is about 12.4 $m^2\ g^{-1}$ smaller than the E. Grandis lignin's 20 $m^2\ g^{-1}$ [15], and the total pore volume is about 1.8 $mL\ g^{-1}$ close to the E. Grandis lignin. Although Klapiszewski et al. reported that the modified lignin was about 0.1 $m^2\ g^{-1}$, and the total pore volume was about only 0.001 $mL\ g^{-1}$.

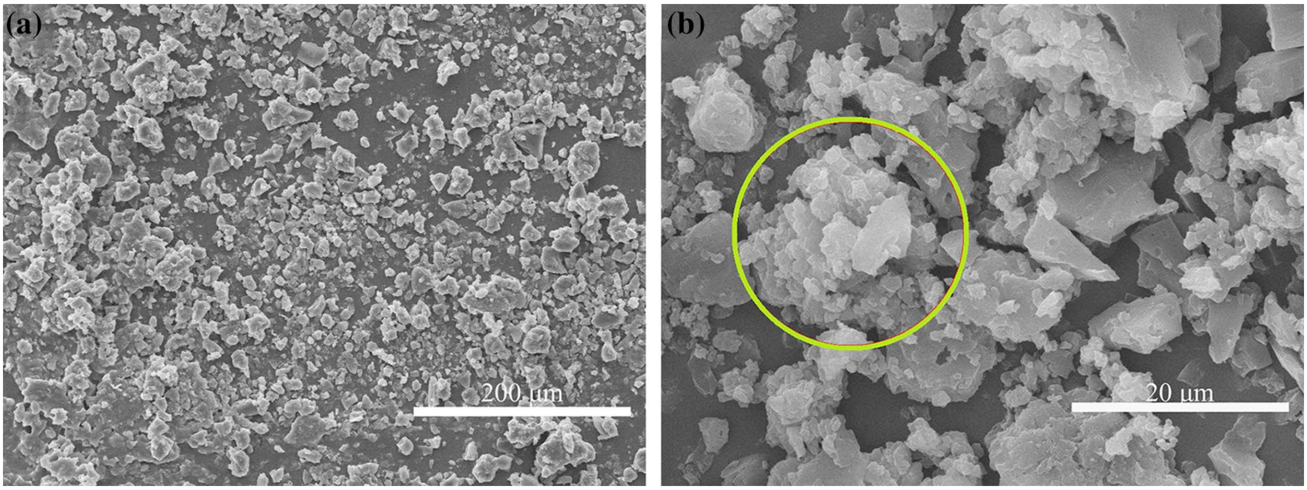

Fig. 8 The morphology of lignin extracted at 220 ℃: **a** 2000 × magnified morphology of stalk lignin; **b** 5000 × magnified morphology of stalk lignin

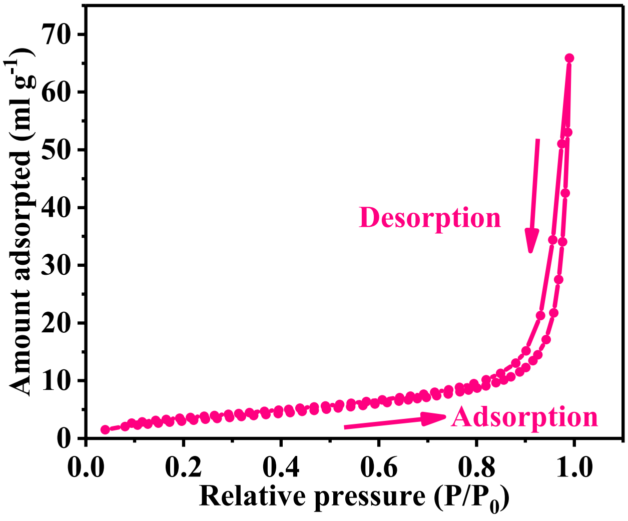

Fig. 9 N_2 adsorption and desorption isotherms lignin sample

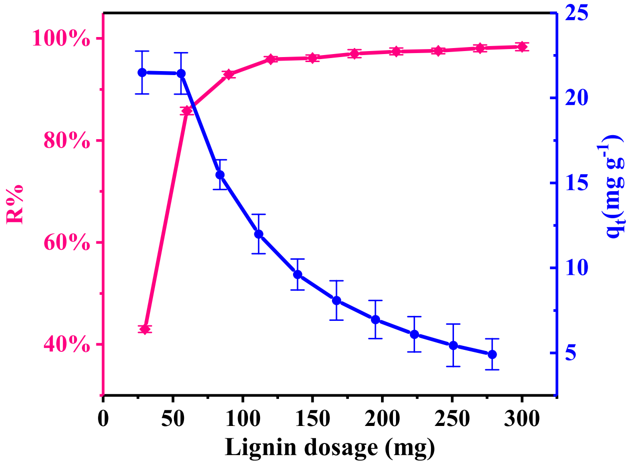

Fig. 10 Influence of the lignin powder dosage on the MB removal performance

Table 6 The pH_{PZC} and specific surface area of cotton stalk lignin

Sample	Specific (m^2 g^{-1})	Total pore volume (mL g^{-1})	pHpzc
Cotton stalk lignin	12.4	1.8	3.26
Modification lignin [68]	0.1	0.001	–
E. grandis lignin [15]	20	2.5	3.15

Adsorption of MB by Cotton Stalk Lignin

The Effect of the Lignin Dosage

Figure 10 is the influence of the lignin dosage on the MB removal performance. The %R curve increases monotonically with increasing dose. This is due to the increased amount of hydroxyl and carboxyl groups in lignin [21]. As the amount of lignin increases, the probability of MB cations contacting lignin increases greatly, which is also one of the reasons for the increase in adsorption capacity. While the q_t curve shows a monotonically decreasing trend with the increasing lignin dosage. The experimental conclusions were consistent with the result reported by Cemin et al. [15].

Isothermal Model for the Adsorption of MB by Lignin

Figure 11 is MB adsorption data of lignin adjusted to the isotherm functions. All curves show a good match with the experimental data. The blue curve represented the

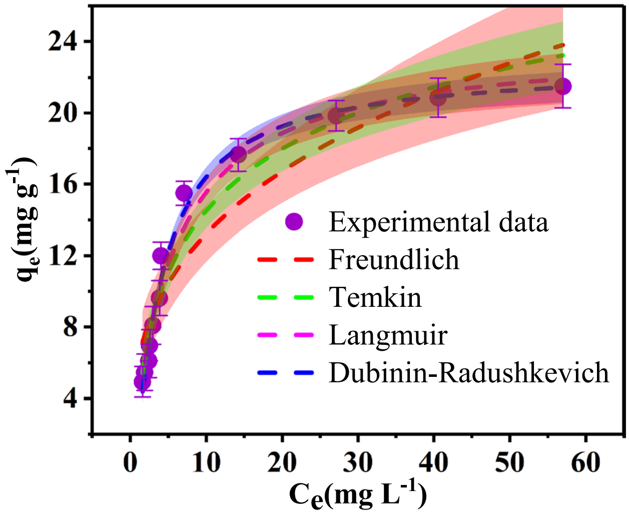

Fig. 11 The MB adsorption data of lignin adjusted to the isotherm functions

Table 7 The parameters of isotherm functions according to the fitting curves of MB adsorption data

Isotherm model	Parameter	Obtained value
Freundlich	k_F (mg g^{-1} (L mg^{-1})$^{1/n}$)	6.07584
	1/n	0.33784
	R^2	0.8769
Langmuir	k_L (L mg^{-1})	0.18314
	q_m (mg g^{-1})	24.0095
	R^2	0.97369
Temkin	A_t (L g^{-1})	495.445
	b_t (J mg^{-1})	1.82165
	R^2	0.95046
	q_s(mg g^{-1})	22.75306
Dubinin–Radushkevich	k_{ad} (mol^2 J^{-2})	1.418E-3
	R^2	0.988

Dubinin–Radushkevich model is the best one that matches the experimental data points, and the pink curve represented Langmuir is the second fit degree one. As shown in Table 7, the R^2 is 0.988, 0.9737, 0.9505, and 0.8769. The variance is also indicated that the Dubinin–Radushkevich model is the best-matching isotherm model which is slightly different from the results of Cemin's and Zou's research, whose isotherm model was Langmuir [15, 61]. According to the assumption of the Dubinin–Radushkevich (DR) model, the surface of the adsorbent is not uniform and the adsorption is by filling the pores. In the above SEM test, we found that the lignin surface was rough, and the specific surface area and pore tests also proved that lignin was a mesoporous material. For the DR model, q_s is the amount of MB adsorbed by lignin, which is 22.7531 mg g^{-1}. While the Langmuir model shows that the maximum adsorption amount of MB by lignin is 24.0095 mg g^{-1}. The k_L of the Langmuir model report here is 0.1831 L mg^{-1} much bigger than Cemin's report (0.0223 L mg^{-1}) [15], but close to Zhang's report (0.2083 L mg^{-1}) [23].

Kinetic Studies

Figure 12 is the MB adsorption of cotton stalk lignin adjusted to the adsorption kinetic equation and the intra-particle diffusion model. Table 8 are the fitting parameters of kinetic equations and internal diffusion. Figure 12a is the matching curve of the pseudo-first-order kinetic equation. The best matching curve is the 170 mg L^{-1} sample, its R^2 is 0.8544, its K_1 value is 0.01657 min^{-1}, and the calculated equilibrium concentration is 35.71 mg/g. All actu$_{al}$ values obtained from Fig. 12a are consistent with the experimental values, but the data in the reaction process greatly deviated from the curve, which is also the reason why the R^2 values are lower. The sample with the highest fitting value in Fig. 12b is also 170 mg L^{-1}, its R^2 is 0.9705, and the calculated equilibrium concentration is 33.99 mg/g, which is lower than the q_{ex} value of 1.72 mg/g. Different from Fig. 12a, all R^2 values are higher than 0.93, which means that the kinetic equation is more inclined to the pseudo-second-order kinetic equation. The conclusion is consistent with the reports of Cemin et al. and Zhang et al.[15, 23].

These experimental data were also used to match the intra-particle diffusion model to predict the rate-limiting step of methylene blue cations adsorbed by lignin particles. Figure 12c is the intra-particle diffusion model. The obtained parameters are also listed in Table 8. All fitted lines have an intercept C, which indicates that the intra-particle diffusion of the adsorption of methylene blue cations was not the only rate-controlled step [62, 63]. The diffusion of MB is divided into two or three stages according to the experimental data. At low concentrations (120 mg L^{-1}, 150 mg L^{-1}), the models are divided into three stages. While slightly higher concentrations of 170 mg L^{-1} and 200 mg L^{-1}, the models are divided into two stages. Regardless of the division method, the slope of the fitted line in the first stage is very large, which indicates that the methylene blue ions are rapidly transferred to the adsorption interface of lignin. The second stage was the real intra-particle diffusion, where methylene blue ions gradually diffused in the mesopores of the lignin [64]. The slope of the fitting line in the third stage begins to decrease, indicating that the particle adsorption process slowly reaches an equilibrium state [63]. The solution with low concentration can show the process of micropore diffusion after a period of diffusion, while the MB solution with high concentration can only show the diffusion process of MB in mesopores.

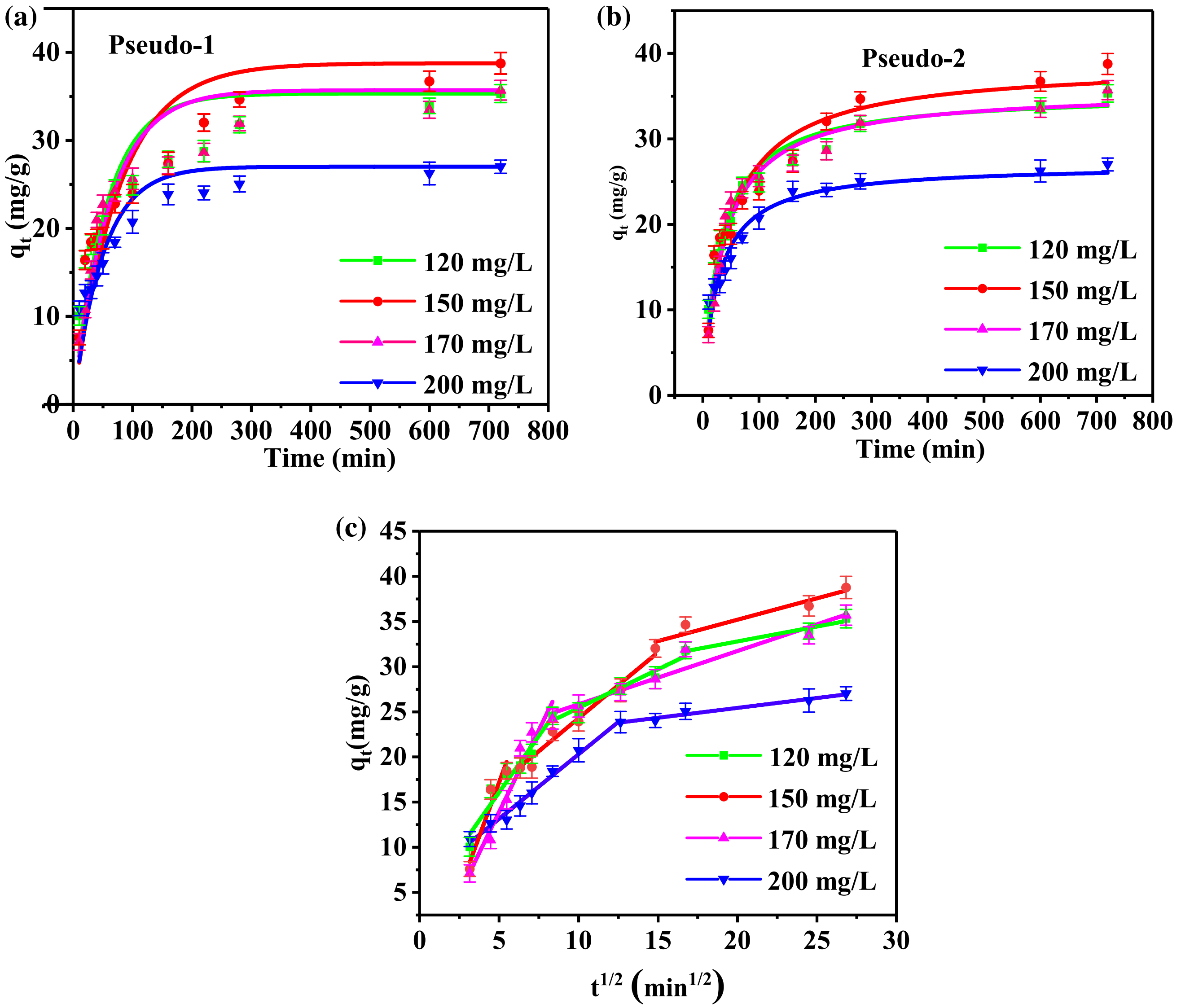

Fig. 12 The fitting of the MB adsorption kinetic study:**a** the pseudo-1 model fitting, **b** the pseudo-2 model fitting, **c** the intra-particle diffusion fitting

Table 8 Kinetic parameters for the linear pseudo-1, pseudo-2, and intra-particle diffusion model

Model	Parameters	Initial concentrations (mg L^{-1})			
		120	150	170	200
Experimental	q_{ex} (mg g^{-1})	35.32	38.76	35.71	27.01
Pseudo-1	k_1 (min^{-1})	1.823E-2	1.307E-2	1.1657E-2	1.995E-2
	q_{cal} (mg g^{-1})	35.32	38.76	35.71	27.01
	R^2	0.7478	0.7899	0.8544	0.7912
Pseudo-2	k_2 (g mg^{-1} min^{-1})	8.98E-4	5.93E-4	7.67E-4	1.35E-3
	q_{cal} (mg g^{-1})	33.84	36.55	33.99	26.02
	R^2	0.9588	0.9436	0.9705	0.9369
Intra-particle diffusion	k_3 (mg g^{-1} $min^{0.5}$)	0.85449	1.46047	0.59051	0.21857
	C (mg g^{-1})	16.88118	9.68129	19.926	21.0626
	R^2	0.94168	0.96999	0.93574	0.96226

q_{ex} is the experiment data of equilibrium q_t value

$q_{(cal)}$ is the calculated q_t value at equilibrium according to the curve

Effect of pH

The MB adsorption influenced by pH is shown in Fig. 13. The graph shows that the suitable pH range for MB sorption by cotton stalk lignin particles is 3–8, and out of the range, the adsorption of lignin particles shows poor performance. The conclusion is following the report of Cemin et al. [15]. When pH equals 7, cotton stalk lignin particles show the best adsorption performance, reaching 17.11 mg/g.

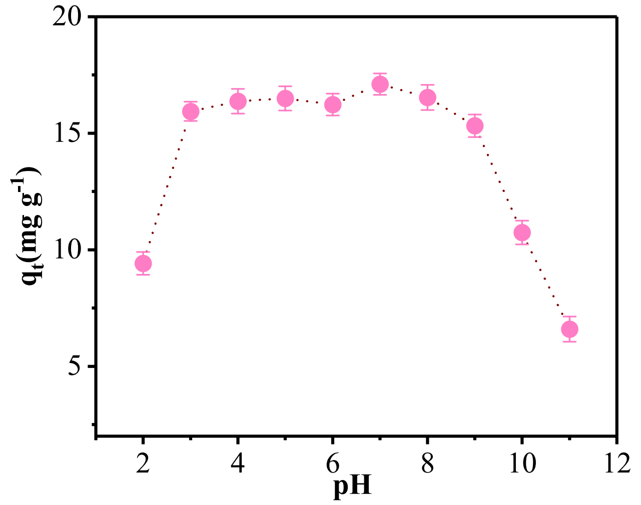

Fig. 13 Effect of pH on the adsorption of MB by lignin

The pH_{PZC} value is 3.26 as shown in Table 6, which means that when the pH < 3.26, lignin exhibits a positively charged nature that is exclusive to the MB cation, so that the MB adsorbability of lignin particles appears to decrease when the solution pH is less than 3 as shown in Fig. 14. Cemin et al. similarly reported that pHpzc was 3.15 which was close to our pH_{PZC}, and they also reported the performance of adsorbed MB showed a decreasing trend when pH < 3 [15]. When the pH was greater than pH_{PZC} (3.26) less than 5.56, the lignin particles exhibited negative charge characteristics and were able to attract MB cations, and when the pH was greater than 5.56, the reason why lignin adsorbed methylene blue was that their aromatic rings formed π bonds [15, 65]. The pH = 5.56 is the critical value for whether methylene blue will develop color or not [66].

Mechanism of Lignin Adsorption of Methylene Blue

AS mentioned above, when the pH > pH_{PZC}, the lignin show a negative charge, and its oxygenated functional groups such as carboxyl and hydroxyl according to FT-IR could interact with the MB molecules through hydrogen bonds,

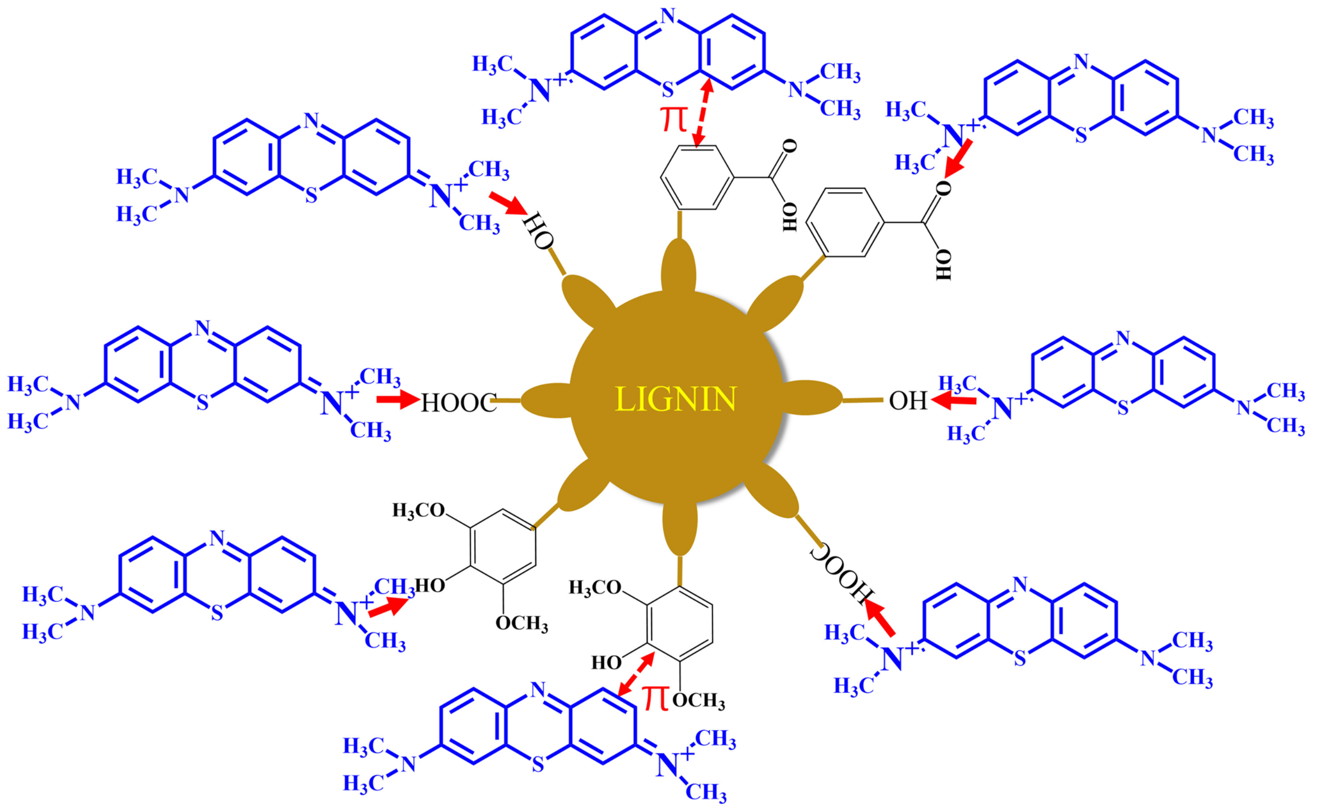

Fig. 14 The adsorption pathway of cotton stalk lignin to methylene blue

which are one of the main intermolecular forces responsible for adsorption [15]. Besides, the aromatic rings in lignin and MB molecular would inform π-π bonds, and favored the adsorption [67]. The adsorption pathway of cotton stalk lignin to methylene blue is shown in Fig. 14.

Conclusions

In this paper, ethanol solution assisted with hot water pretreatment was used to extract lignin from cotton stalks. The removal rate of hemicellulose was 93.26%, and the lignin yield was 15.65% with around 900 Da. The TGA test showed that the thermal degradation process of cotton stalk lignin was divided into three stages according to the degradation rates, and 230 ℃ was the fastest degradation temperature. FT-IR and 2D-NMR showed that the cotton stalk lignin was the typical grass lignin that contained lots of G, S, and H units. The SEM proved that there were a large number of burr structures on the surface of the block lignin, which was consistent with the conclusion that lignin had a mesoporous structure by the subsequent N_2 adsorption test. In the experiment of lignin used in the adsorption of methylene blue, the best adsorption isotherm model matching its experimental data is the DR model, the variance was 0.988 and the pseudo-second-order kinetic equation was the best matching kinetic equation to match the experimental data, the optimal variance reached 0.9705 and the intra- particle diffusion occurs in the second stage of fitting the polyline, the optimal variance reached 0.97. The pH range suitable for lignin adsorption of methylene blue is 3–8.

Acknowledgements This work was supported by the National Natural Science Foundation of China (No. 21706026)

Author Contributions Conceptualization: XW, FL, ZL; Methodology: TY, ZL; Formal analysis and investigation: TY, XX; Writing—original draft preparation: TY; Writing—review and editing: ZL, ZL; Funding acquisition: XW; Resources: WW; Supervision: WW, XX.

Funding This work was supported by the National Natural Science Foundation of China (Grant No*:* [21706026]).

Data Availability The datasets generated during and/or analysed during the current study are available in the [manuscript],[taary materials] repository.

Declarations

Conflict of interest The authors have no relevant financial or non-financial interests to disclose.

References

1. Luong, N.D., Binh, N.T.T., Duong, L.D., Kim, D.O., Kim, D.S., Lee, S.H., Kim, B.J., Lee, Y.S., Nam, J.: Do: an eco-friendly and efficient route of lignin extraction from black liquor and a lignin-based copolyester synthesis. Polym. Bull. **68**, 879–890 (2012). https://doi.org/10.1007/s00289-011-0658-x
2. Sarkanen, K.V., Islam, A., Anderson, C.D.: Methods in Lignin Chemistry. In: Lin, S.Y. and Dence, C.W. (eds.) Springer Series in Wood Science. pp. 387–406. Springer Berlin Heidelberg (1992)
3. Cheng, H.N., Dowd, M.K., Shogren, R.L., Biswas, A.: Conversion of cotton byproducts to mixed cellulose esters. Carbohydr. Polym. **86**, 1130–1136 (2011). https://doi.org/10.1016/j.carbpol.2011.06.002
4. Apaydin-Varol, E., Uzun, B.B., Önal, E., Pütün, A.E.: Synthetic fuel production from cottonseed: fast pyrolysis and a TGA/FT-IR/MS study. J. Anal. Appl. Pyrolysis **105**, 83–90 (2014). https://doi.org/10.1016/j.jaap.2013.10.006
5. Chen, J., Liang, J., Wu, S.: Lignin-rich biomass of cotton by-products for biorefineries via pyrolysis. Bioresour. Technol. **218**, 402–409 (2016). https://doi.org/10.1016/j.biortech.2016.06.122
6. Luo, Y., Li, Z., Li, X., Liu, X., Fan, J., Clark, J.H., Hu, C.: The production of furfural directly from hemicellulose in lignocellulosic biomass: a review. Catal. Today **319**, 14–24 (2019). https://doi.org/10.1016/j.cattod.2018.06.042
7. Yi, G., Zhang, Y.: One-Pot Selective Conversion of Hemicellulose (Xylan) to Xylitol under Mild Conditions. ChemSusChem. 5, 1383–1387 (2012). https://doi.org/10.1002/cssc.201200290
8. Wang, L., Li, T., Liu, F., Liu, D., Xu, Y., Yang, Y., Zhao, Y., Wei, H.: Ultrasonic-assisted enzymatic extraction and characterization of polysaccharides from dandelion (*Taraxacum officinale*) leaves. Int. J. Biol. Macromol. **126**, 846–856 (2019). https://doi.org/10.1016/j.ijbiomac.2018.12.232
9. Otieno, D.O., Ahring, B.K.: The potential for oligosaccharide production from the hemicellulose fraction of biomasses through pretreatment processes: xylooligosaccharides (XOS), arabinooligosaccharides (AOS), and mannooligosaccharides (MOS). Carbohydr. Res. **360**, 84–92 (2012). https://doi.org/10.1016/j.carres.2012.07.017
10. Hansen, N.M.L., Plackett, D.: Sustainable films and coatings from hemicelluloses: a review. Biomacromol **9**, 1493–1505 (2008). https://doi.org/10.1021/bm800053z
11. Civelek Yoruklu, H., Koroglu, E.O., Ozdemir, O.K., Demir, A., Ozkaya, B.: Bioenergy production from cotton straws using different pretreatment methods. Int. J. Hydrog. Energy. **45**, 34720–34729 (2020). https://doi.org/10.1016/j.ijhydene.2020.02.104
12. Dai, L., Cheng, T., Duan, C., Zhao, W., Zhang, W., Zou, X., Aspler, J., Ni, Y.: 3D printing using plant-derived cellulose and its derivatives: a review. Carbohydr. Polym. **203**, 71–86 (2019). https://doi.org/10.1016/j.carbpol.2018.09.027
13. Zhifeng, Z.: Research Progress in Cellulose Degradation by Cellulase. Chem. Ind. Eng. Prog. 29, 1493–1501 (2016).https://doi.org/10.14159/j.cnki.0441-3776.2016.02.004 https://urldefense.com/v3/
14. Dorrestijn, E., Laarhoven, L.J.J., Arends, I.W.C.E., Mulder, P.: Occurrence and reactivity of phenoxyl linkages in lignin and low rank coal. J. Anal. Appl. Pyrolysis **54**, 153–192 (2000). https://doi.org/10.1016/S0165-2370(99)00082-0
15. Cemin, A., Ferrarini, F., Poletto, M., Bonetto, L.R., Bortoluz, J., Lemée, L., Guégan, R., Esteves, V.I., Giovanela, M.: Characterization and use of a lignin sample extracted from *Eucalyptus grandis* sawdust for the removal of methylene blue dye. Int. J. Biol. Macromol. **170**, 375–389 (2021). https://doi.org/10.1016/j.ijbiomac.2020.12.155
16. Gómez-Ceballos, V., García-Córdoba, A., Zapata-Benabithe, Z., Velásquez, J., Quintana, G.: Preparation of hyperbranched polymers from oxidized lignin modified with triazine for removal of heavy metals. Polym. Degrad. Stab. (2020). https://doi.org/10.1016/j.polymdegradstab.2020.109271

17. Wang, B., Sun, Y.-C., Sun, R.-C.: Fractionational and structural characterization of lignin and its modification as biosorbents for efficient removal of chromium from wastewater: a review. J. Leather Sci. Eng. **1**, 1–25 (2019). https://doi.org/10.1186/s42825-019-0003-y
18. Ben Mosbah, M., Mechi, L., Khiari, R., Moussaoui, Y.: Current state of porous carbon for wastewater treatment. Processes (2020). https://doi.org/10.3390/pr8121651
19. Taleb, F., Ammar, M., Mosbah, M., ben Salem, R., Moussaoui, Y.: Chemical modification of lignin derived from spent coffee grounds for methylene blue adsorption. Sci. Rep. **10**, 1–13 (2020). https://doi.org/10.1038/s41598-020-68047-6
20. Supanchaiyamat, N., Jetsrisuparb, K., Knijnenburg, J.T.N., Tsang, D.C.W., Hunt, A.J.: Lignin materials for adsorption: current trend, perspectives, and opportunities. Bioresour. Technol. **272**, 570–581 (2019). https://doi.org/10.1016/j.biortech.2018.09.139
21. Jin, Y., Zeng, C., Lü, Q.F., Yu, Y.: Efficient adsorption of methylene blue and lead ions in aqueous solutions by 5-sulfosalicylic acid modified lignin. Int. J. Biol. Macromol. **123**, 50–58 (2019). https://doi.org/10.1016/j.ijbiomac.2018.10.213
22. Yu, C., Wang, F., Zhang, C., Fu, S., Lucia, L.A.: The synthesis and absorption dynamics of a lignin-based hydrogel for remediation of cationic dye-contaminated effluent. React. Funct. Polym. **106**, 137–142 (2016). https://doi.org/10.1016/j.reactfunctpolym.2016.07.016
23. Zhang, S., Wang, Z., Zhang, Y., Pan, H., Tao, L.: Adsorption of methylene blue on organosolv lignin from rice straw. Procedia Environ. Sci. **31**, 3–11 (2016). https://doi.org/10.1016/j.proenv.2016.02.001
24. Shattar, S.F.A., Foo, K.Y.: Sodium salt-assisted low temperature activation of bentonite for the adsorptive removal of methylene blue. Sci. Rep. **12**, 1–12 (2022). https://doi.org/10.1038/s41598-022-06254-z
25. Shittu, I., Achazhiyath Edathil, A., Alsaeedi, A., Al-Asheh, S., Polychronopoulou, K., Banat, F.: Development of novel surfactant functionalized porous graphitic carbon as an efficient adsorbent for the removal of methylene blue dye from aqueous solutions. J. Water Process Eng. **28**, 69–81 (2019). https://doi.org/10.1016/j.jwpe.2019.01.001
26. Zhou, Y., Lu, J., Zhou, Y., Liu, Y.: Recent advances for dyes removal using novel adsorbents: a review. Environ. Pollut. **252**, 352–365 (2019). https://doi.org/10.1016/j.envpol.2019.05.072
27. Dabagh, A., Bagui, A., Abali, M., Aziam, R., Chiban, M., Sinan, F., Zerbet, M.: Increasing the adsorption efficiency of methylene blue by acid treatment of the plant *Carpobrotus edulis*. Chem. Afr. **4**, 585–598 (2021). https://doi.org/10.1007/s42250-021-00233-z
28. Ben Mosbah, M., Alsukaibi, A.K., Mechi, L., Alimi, F., Moussaoui, Y.: Ecological synthesis of CuO nanoparticles using *Punica granatum* L. peel extract for the retention of methyl green. Water (2022). https://doi.org/10.3390/w14091509
29. Elhleli, H., Mannai, F., Ben Mosbah, M., Khiari, R., Moussaoui, Y.: Biocarbon derived from *Opuntia ficus* indica for p-nitrophenol retention. Processes (2020). https://doi.org/10.3390/pr8101242
30. Ouni, A., Rabaaoui, N., Mechi, L., Enaceur, N., AlSukaibi, A.K.D., Azzam, E.M., Alenezi, K.M., Moussaoui, Y.: Removal of pesticide chlorobenzene by anodic degradation: variable effects and mechanism. J. Saudi Chem. Soc. **25**, 101326 (2021). https://doi.org/10.1016/j.jscs.2021.101326
31. Crini, G.: Non-conventional low-cost adsorbents for dye removal: a review. Bioresour. Technol. **97**, 1061–1085 (2006). https://doi.org/10.1016/j.biortech.2005.05.001
32. Hou, Y., Yan, S., Huang, G., Yang, Q., Huang, S., Cai, J.: Fabrication of N-doped carbons from waste bamboo shoot shell with high removal efficiency of organic dyes from water. Bioresour. Technol. **303**, 122939 (2020). https://doi.org/10.1016/j.biortech.2020.122939
33. de Araújo Padilha, C.E., da Costa Nogueira, C., de Santana Souza, D.F., de Oliveira, J.A., dos Santos, E.S.: Organosolv lignin/Fe3O4 nanoparticles applied as a β-glucosidase immobilization support and adsorbent for textile dye removal. Ind. Crops Prod. **146**, 112167 (2020). https://doi.org/10.1016/j.indcrop.2020.112167
34. Shuai, L., Amiri, M.T., Questell-Santiago, Y.M., Héroguel, F., Li, Y., Kim, H., Meilan, R., Chapple, C., Ralph, J., Luterbacher, J.S.: Formaldehyde stabilization facilitates lignin monomer production during biomass depolymerization. Science **354**, 329–333 (2016). https://doi.org/10.1126/science.aaf7810
35. Saber, M., El Hamdaoui, L., El Moussaouiti, M., Tabyaoui, M.: Extraction and characterization of lignin from Moroccan Thuya. Its application as adsorbent of methylene blue from aqueous solution. Cellul. Chem. Technol. **56**, 69–81 (2022). https://doi.org/10.3812/CelluloseChemTechnol.2022.56.06
36. Feng, N., Ren, L., Wu, H., Wu, Q., Xie, Y.: New insights on structure of lignin-carbohydrate complex from hot water pretreatment liquor. Carbohydr. Polym. **224**, 115130 (2019). https://doi.org/10.1016/j.carbpol.2019.115130
37. Giummarella, N., Zhang, L., Henriksson, G., Lawoko, M.: Structural features of mildly fractionated lignin carbohydrate complexes (LCC) from spruce. RSC Adv. **6**, 42120–42131 (2016). https://doi.org/10.1039/c6ra02399a
38. Steinbach, D., Kruse, A., Sauer, J.: Pretreatment technologies of lignocellulosic biomass in water in view of furfural and 5-hydroxymethylfurfural production- a review. Biomass Convers. Biorefinery. **7**, 247–274 (2017). https://doi.org/10.1007/s13399-017-0243-0
39. Trajano, H.L., Engle, N.L., Foston, M., Ragauskas, A.J., Tschaplinski, T.J., Wyman, C.E.: The fate of lignin during hydrothermal pretreatment. Biotechnol. Biofuels **6**, 1–16 (2013). https://doi.org/10.1186/1754-6834-6-110
40. Sun, Y.C., Wen, J.L., Xu, F., Sun, R.C.: Fractional and structural characterization of organosolv and alkaline lignins from Tamarix austromogoliac. Sci. Res. Essays **5**, 3850–3864 (2010)
41. Michelin, M., Liebentritt, S., Vicente, A.A., Teixeira, J.A.: Lignin from an integrated process consisting of liquid hot water and ethanol organosolv: physicochemical and antioxidant properties. Int. J. Biol. Macromol. **120**, 159–169 (2018). https://doi.org/10.1016/j.ijbiomac.2018.08.046
42. Van Soest, P.J., Robertson, J.B., Lewis, B.A.: Methods for dietary fiber, neutral detergent fiber, and nonstarch polysaccharides in relation to animal nutrition. J. Dairy Sci. **74**, 3583–3597 (1991). https://doi.org/10.3168/jds.S0022-0302(91)78551-2
43. Foo, K.Y., Hameed, B.H.: Insights into the modeling of adsorption isotherm systems. Chem. Eng. J. **156**, 2–10 (2010). https://doi.org/10.1016/j.cej.2009.09.013
44. Freundlich, H.: Over the Adsorption in Solution. J. Phys. Chem. A. 57U, 385–470 (1907).https://urldefense.com/v3/. https://doi.org/10.1515/zpch-1907-5723
45. Langmuir, I.: The constitution and fundamental properties of solids and liquids. J. Franklin Inst. **183**, 102–105 (1917). https://urldefense.com/v3/. https://doi.org/10.1016/S0016-0032(17)90938
46. Lagergren, S.: About the Theory of So-Called Adsorption of Soluble Substances. K. Sven. Vetenskapsakademiens Handl **24**, 1–39 (1898)
47. Blanchard, G., Maunaye, M., Martin, G.: Removal of heavy metals from waters by means of natural zeolites. Water Res. **18**, 1501–1507 (1984). https://doi.org/10.1016/0043-1354(84)90124-6
48. Khadhri, N., El Khames Saad, M., Ben Mosbah, M., Moussaoui, Y.: Batch and continuous column adsorption of indigo carmine onto activated carbon derived from date palm petiole. J. Environ. Chem. Eng. **7**, 102775 (2019). https://doi.org/10.1016/j.jece.2018.11.020
49. Kumar, A., Jena, H.M.: Adsorption of Cr(VI) from aqueous solution by prepared high surface area activated carbon from Fox

nutshell by chemical activation with H3PO4. J. Environ. Chem. Eng. **5**, 2032–2041 (2017). https://doi.org/10.1016/j.jece.2017.03.035

50. Yang, T., Li, Z., Wei, W., Wang, X., Liu, F., Xu, X., Liu, Z.: Antioxidant properties of lignin extracted from cotton stalks by ethanol solution-assisted liquid hot water before and after adding supercritical CO2. J. CO2 Util. **58**, 1892 (2022). https://doi.org/10.1016/j.jcou.2022.101892
51. Lei, M., Zhang, H., Zheng, H., Li, Y., Huang, H., Xu, R.: Characterization of lignins isolated from alkali treated prehydrolysate of corn stover. Chin. J. Chem. Eng. **21**, 427–433 (2013). https://doi.org/10.1016/S1004-9541(13)60468-1
52. Sun, Y., Wang, T., Han, C., Lv, X., Bai, L., Sun, X., Zhang, P.: Facile synthesis of Fe-modified lignin-based biochar for ultra-fast adsorption of methylene blue: selective adsorption and mechanism studies. Bioresour. Technol. **344**, 126186 (2022). https://doi.org/10.1016/j.biortech.2021.126186
53. Faix, O.: Classification of lignins from different botanical origins by FT-IR spectroscopy. Holzforschung **45**, 21–28 (1991). https://doi.org/10.1515/hfsg.1991.45.s1.21
54. Yang, H., Yan, R., Chen, H., Lee, D.H., Liang, D.T., Zheng, C.: Mechanism of palm oil waste pyrolysis in a packed bed. Energy Fuels **20**, 1321–1328 (2006). https://doi.org/10.1021/ef0600311
55. de Oliveira Simões Saliba, E., Rodriguez, N.M., de Antônio Lemos Morais, S., Piló-Veloso, D.: Ligninas: métodos de obtenção e caracterização química. Ciência Rural **31**, 917–928 (2001). https://doi.org/10.1590/s0103-84782001000500031
56. Wei, Y.N., Liu, H.M., Fu, C.Q., Qin, Z., Wang, C.Y., Yang, M.X., He, J.: Structural changes for lignin from Chinese quince during the sequential fractionation of cell wall polysaccharides. Process Biochem. **113**, 167–176 (2022). https://doi.org/10.1016/j.procbio.2021.12.033
57. Del Río, J.C., Rencoret, J., Marques, G., Li, J., Gellerstedt, G., Jesús, J.B., Martínez, A.T., Gutiérrez, A.N.A.: Structural characterization of the lignin from jute (*Corchorus capsuiaris*) fibers. J. Agric. Food Chem. **57**, 10271–10281 (2009). https://doi.org/10.1021/jf900815x
58. Rinaldi, R., Jastrzebski, R., Clough, M.T., Ralph, J., Kennema, M., Bruijnincx, P.C.A., Weckhuysen, B.M.: Paving the way for lignin valorisation: recent advances in bioengineering, biorefining and catalysis. Angew. Chem.—Int. Ed. **55**, 8164–8215 (2016). https://doi.org/10.1002/anie.201510351
59. Ralph, S., Ralph, J., Landucci, L., Service, U.F., Ralph, J.: NMR database of lignin and cell wall model compounds (2009). https://urldefense.com/v3. https://www.glbrc.org/databases_and_software/nmrdatabase/NMR_DataBase_2009_Intro_and_Structure-Index.pdf
60. Thommes, M., Kaneko, K., Neimark, A.V., Olivier, J.P., Rodriguez-Reinoso, F., Rouquerol, J., Sing, K.S.W.: Physisorption of gases, with special reference to the evaluation of surface area and pore size distribution (IUPAC Technical Report). Pure Appl. Chem. **87**, 1051–1069 (2015). https://doi.org/10.1515/pac-2014-1117
61. Zou, W., Bai, H., Gao, S., Li, K.: Characterization of modified sawdust, kinetic and equilibrium study about methylene blue adsorption in batch mode. Korean J. Chem. Eng. **30**, 111–122 (2013). https://doi.org/10.1007/s11814-012-0096-y
62. Xie, A., Dai, J., Chen, X., Ma, P., He, J., Li, C., Zhou, Z., Yan, Y.: Ultrahigh adsorption of typical antibiotics onto novel hierarchical porous carbons derived from renewable lignin via halloysite nanotubes-template and in-situ activation. Chem. Eng. J. **304**, 609–620 (2016). https://doi.org/10.1016/j.cej.2016.06.138
63. Tan, Y., Wang, X., Xiong, F., Ding, J., Qing, Y., Wu, Y.: Preparation of lignin-based porous carbon as an efficient absorbent for the removal of methylene blue. Ind. Crops Prod. **171**, 113980 (2021). https://doi.org/10.1016/j.indcrop.2021.113980
64. Wang, A., Zheng, Z., Li, R., Hu, D., Lu, Y., Luo, H., Yan, K.: Biomass-derived porous carbon highly efficient for removal of Pb(II) and Cd(II). Green Energy Environ. **4**, 414–423 (2019). https://doi.org/10.1016/j.gee.2019.05.002
65. Garg, V.K., Gupta, R., Yadav, A.B., Kumar, R.: Dye removal from aqueous solution by adsorption on treated sawdust. Bioresour. Technol. **89**, 121–124 (2003). https://doi.org/10.1016/S0960-8524(03)00058-0
66. Scotti, R., Lima, E.C., Benvenutti, E.V., Piatnicki, C.M.S., Dias, S.L.P., Gushikem, Y., Kubota, L.T.: Azul de metileno imobilizado na celulose/TiO2 e SiO 2/TiO2: propriedades eletroquímicas e planejamento fatorial. Quim. Nova **29**, 208–212 (2006). https://doi.org/10.1590/S0100-40422006000200006
67. Alidadi, H., Dolatabadi, M., Davoudi, M., Barjasteh-Askari, F., Jamali-Behnam, F., Hosseinzadeh, A.: Enhanced removal of tetracycline using modified sawdust: Optimization, isotherm, kinetics, and regeneration studies. Process Saf. Environ. Prot. **117**, 51–60 (2018). https://doi.org/10.1016/j.psep.2018.04.007
68. Klapiszewski, Ł, Wysokowski, M., Majchrzak, I., Szatkowski, T., Nowacka, M., Siwińska-Stefańska, K., Szwarc-Rzepka, K., Bartczak, P., Ehrlich, H., Jesionowski, T.: Preparation and characterization of multifunctional chitin/lignin materials. J. Nanomater. (2013). https://doi.org/10.1155/2013/425726

Publisher's Note Springer Nature remains neutral with regard to jurisdictional claims in published maps and institutional affiliations.

Springer Nature or its licensor (e.g. a society or other partner) holds exclusive rights to this article under a publishing agreement with the author(s) or other rightsholder(s); author self-archiving of the accepted manuscript version of this article is solely governed by the terms of such publishing agreement and applicable law.